

Imidazole-2-carboxaldehyde Chitosan Thiosemicarbazones and their Copper(II) Complexes: Synthesis, Characterization and Antitumorigenic Activity against Madin-Darby Canine Kidney Cell Line

HARI SHARAN ADHIKARI^{1,✉}, ADITYA GARAI^{2,✉}, CHETANA KHANAL^{3,✉}, RAMESHWAR ADHIKARI^{4,5,✉} and PARAS NATH YADAV^{5,*✉}

¹Institute of Engineering, Pashchimanchal Campus, Department of Applied Sciences, Tribhuvan University, Pokhara, Nepal

²Department of Inorganic and Physical Chemistry, Indian Institute of Science, Bangalore-560012, India

³Central Department of Biotechnology, Tribhuvan University, Kathmandu, Nepal

⁴Research Centre for Applied Science and Technology (RECAST), Tribhuvan University, Kathmandu, Nepal

⁵Central Department of Chemistry, Tribhuvan University, Kathmandu, Nepal

*Corresponding author: E-mail: pnyadav219@gmail.com

Received: 24 November 2020;

Accepted: 3 February 2021;

Published online: 16 April 2021;

AJC-20312

Chitosan oligosaccharide and high molecular weight crab shell chitosan were functionalized as imidazole-2-carboxaldehyde chitosan thiosemicarbazones and their copper(II) complexes were synthesized. The synthesized compounds were characterized by FT-IR, ¹³C NMR, EPR spectroscopy, powder X-ray diffraction (PXRD) analysis, elemental analysis and magnetic susceptibility measurements. The low molecular weight chitosan thiosemicarbazones showed higher *in vitro* inhibitory activity as studied by MTT assay against the tumorigenic epithelial Madin-Darby Canine Kidney (MDCK) cell line than the corresponding high molecular weight chitosan derivative. The antitumorigenic enhancement upon the complex formation was revealed by the better inhibitory activity of copper(II) chitosan thiosemicarbazone chelates.

Keywords: Antitumorigenic activity, Chitosan thiosemicarbazones, Imidazole-2-carboxaldehyde, MDCK cell line.

INTRODUCTION

Chitin is a natural polymer of D-glucosamine units connected by β -(1-4)-linkages and chitosan is a polymer of N-acetyl D-glucosamine units obtained by a prolonged deacetylation of chitin (Fig. 1) with alkali [1]. Chitosan undergoes protonation in C2 position of glucosamine ring and gets dissolved in aqueous acidic media [1].

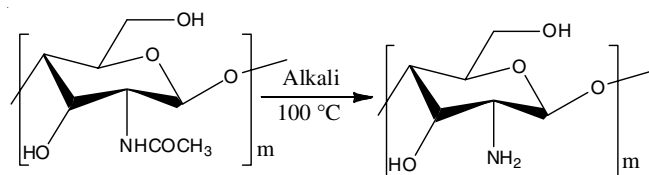


Fig. 1. Deacetylation of chitin into chitosan

Chemical modification involving the primary and secondary hydroxyl and amino groups in pyranose ring of chitosan can give different compounds of industrial and biomedical

applications [2,3]. Chitosan tailoring with the involvement of reactive hydroxy groups and amino and acetamido moieties can bring about the derivatives of enhanced solubility and anti-cancer activity [4]. Chitosan can be functionalized to get bio-active Schiff base derivatives with the compounds containing carbonyl moiety such as maltol [5], imidazole-2-carboxaldehyde and thiophene-2-carboxaldehyde [6] and salicylaldehyde [7].

Chitosan has been reported as an anticancer agent with minimal toxicity on noncancer cells [8] and its activity against the proliferation of tumour cell lines has been found to increase with decrease in molecular weight (M_w) and increase in degree of deacetylation (DDA) [9]. Chitosan shows coordination behaviour with cupric ions to give the complexes of antitumor activity that is associated with increase in positive charge in amino group of chitosan and easier interaction with negatively charged cell surfaces [10]. Chitosan thiosemicarbazones are the functional derivatives of chitosan that show antioxidant ability to scavenge and minimize the formation of immunosuppressive and cancer-causing free radicals [11-13] and their antioxidant behaviour

is due to abstraction of proton from amino and hydroxyl groups in C-2, C-3 and C-6 positions of pyranose ring by free radicals [14]. Introduction of thiosemicarbazone group to chitosan has been reported to weaken the intramolecular and intermolecular hydrogen bonds and cause an increase in interaction of N-H and C=S groups with free radicals. Antiproliferative activity of chitosan thiosemicarbazones could be attributed to degradation of free radicals due to interaction with antioxidant entities [4,11].

The imidazole based anticancer drugs have been found to interfere with the synthesis of deoxyribonucleic acid (DNA) followed by the cease of cell growth and division [15]. The anticancer activity of thiosemicarbazones has been reported to be attributed to different modes of action, such as inhibition in the synthesis of DNA by inhibition of ribonucleotide reductase (RR), inhibition of cellular iron up take, generation of reactive oxygen species (ROS), up regulation of metastasis suppressor protein, inhibition of topoisomerase, induction of apoptosis [16] and the antiausterity behaviour to diminish the tolerance of cancer cells in austere environment of nutrient starvation [17]. The coordination of copper with thiosemicarbazone has been shown to increase the cytotoxic effect [18-21] and DNA inhibition capacity of uncoordinated thiosemicarbazones [18]. Anticancer activity of imidazole-derived thiosemicarbazones was enhanced upon their copper(II) complex formation [22].

The neoplastic development of cultured Madin-Darby Canine Kidney (MDCK) cells has been shown by *in vitro* expression of immortalized cells as tumorigenic phenotype from commercially available normal kidney cells [23]. Chitosan oligosaccharide at a concentration of 100-500 µg/mL has been reported to inhibit the formation and growth of MDCK cyst model [24] and chemical modification through functionalization and complex formation has been shown to bring enhancement in permeation through plasma membrane and cellular cytotoxicity [4]. On the basis of these literature reports, present current work was focused on the synthesis of imidazole-2-carboxaldehyde based novel chitosan thiosemicarbazones and their copper(II) complexes and the assessment of their anti-proliferative activity against the tumorigenic epithelial Madin-Darby Canine Kidney (MDCK) cell line *in vitro*.

EXPERIMENTAL

Chitosan oligosaccharide, $(C_{12}H_{24}N_2O_9)_n$ ($M_w < 3000$ Da, 87% DDA) (Sisco Research Lab. Pvt. Ltd., India), imidazole-2-carboxaldehyde (Sigma-Aldrich), ethanol (Sigma-Aldrich, 99.80%), glacial acetic acid (Merck, 99-100%), hydrochloric acid (Merck, 99%), sodium hydroxide (Merck, 99%), sodium

acetate (Merck), copper(II) chloride (Merck), sodium chloroacetate, acetone, hydrazine monohydrate (Thermo-Fisher Scientific), carbon disulphide (S.D. Fine-Chem Ltd.), methanol, ammonium hydroxide and all other chemical reagents of analytical grade were used without further purification.

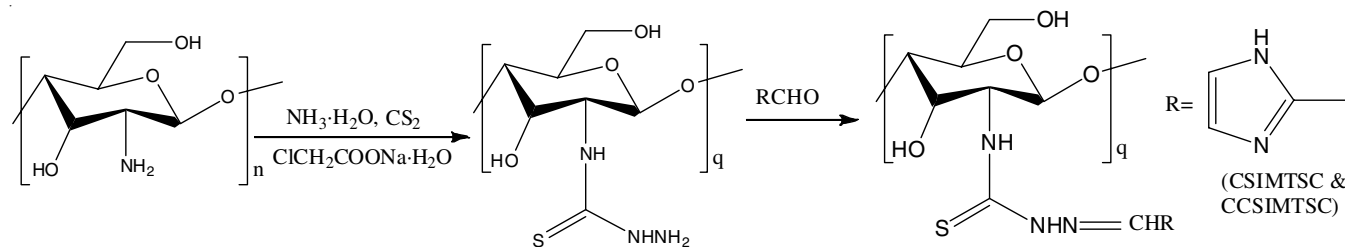
Characterization: The FT-IR spectra were recorded in the 4000-400 cm^{-1} regions with ATR-GeXPm experimentation using BRUKER 3610 FT-IR spectrophotometer. Solid state ^{13}C NMR spectra were recorded using BRUKER AC-800 Delta 2 NMR spectrometer with cross polarization at a field strength (400 MHz), scans 276 and contact time of 3.5 min. Powder X-ray diffraction (PXRD) was done at D8 advance BRUKER diffractometer ($\lambda = 0.1541$ nm) at 40 KV, the particle size (D) was determined from Debye-Scherrer formula [25] and crystallinity index was determined from the intensities of maximum intensity peak and adjacent amorphous diffraction [26]. The elemental analyses were conducted on the Thermo-Finnigan FLASH EA 112CHNS microanalyzer with carrier gas He (140 mL/min) using CHNS/NCS column PQS SS 2M 6X5 mm in oven at 75 °C.

The thermal analyses (TG/DTA/DTG) were conducted on the Model- SII 6300 EXSTAR at IIT Roorkee India. The EPR spectra were recorded using Bruker biospin corp. (EMX series) Model: A 200-9.5/12B/S. The FT-IR, ^{13}C NMR, PXRD, elemental analyses, magnetic moment measurements were carried out at Indian Institute of Science, Bangalore, India.

Functionalization of chitosan as chitosan thiosemicarbazide: A mixture of 2 g of chitosan and 2.5 mL of ammonium hydroxide in absolute ethanol was stirred at room temperature for 1 h. Carbon disulphide (1 mL) was added in drops and the mixture was stirred for 2.5 h. Next, sodium chloroacetate (1.437 g) was added, stirred at room temperature for 2.5 h, the resulting mixture was filtered, residue was completely washed with absolute ethanol and left overnight at 40 °C to get a light brown powder of chitosan thiosemicarbazide [27].

Synthesis of chitosan thiosemicarbazones: Synthetic route of chitosan thiosemicarbazones (**Scheme-I**) involved a reflux condensation of an equimolar mixture of 2 mmol each of chitosan thiosemicarbazide and imidazole-2-carboxaldehyde at 65 °C for 12 h in methanol in the presence of acetic acid as catalyst. After filtration, the residue was washed with methanol and dried overnight at 40 °C [27,28].

Imidazole-2-carboxaldehyde oligo chitosan thiosemicarbazone (CSIMTSC): Yield: 73 %; colour: yellowish brown; m.p. > 300 °C, decomposed into brown residue prior to melting; calcd. for $C_{11}H_{15}N_5O_4S$ (unit formula wt. 313.35, chitosan unit 160.16) C, 41.90; H, 5.43; N, 22.21; S, 10.17 %; found (for



Scheme-I: Synthetic route of chitosan thiosemicarbazones

87% DDA of chitosan) C, 40.30; H, 5.07; N, 23.75; S, 3.61%; DS: 22.63%.

Imidazole-2-carboxaldehyde crab chitosan thiosemicarbazone (CCSIMTSC): Yield: 71 %; colour: yellowish brown; m.p. > 300 °C, decomposed prior to melting; calcd. for C₁₁H₁₅N₅O₄S (unit formula wt. 313.35, chitosan unit 160.16) C, 41.90; H, 5.43; N, 22.21; S, 10.17%; found (for 67 % DDA of chitosan) C, 40.16; H, 7.10; N, 19.05; S, 3.2%; DS: 20.18%.

Synthesis of copper(II) chitosan thiosemicarbazones:

The copper(II) to ligand (1:1) complexes were synthesized as novel compounds with some modifications in the literature method by Wang *et al.* [29]. An equimolar mixture of 2 mmol each of chitosan thiosemicarbazone and copper(II) chloride was dissolved in 15 mL of 1% acetic acid solution, pH of the mixture was maintained at 6 by addition of 5% NaOH solution in little instalments. The resulting solution was stirred for 3 h at 60 °C, filtered and the complex obtained as residue was dried overnight at 40 °C.

Copper(II) imidazole-2-carboxaldehyde oligo chitosan thiosemicarbazone (Cu-CSIMTSC): Yield: 78%; colour: greenish yellow; m.p. > 300°C, decomposed prior to melting; calcd. for C₁₁H₁₅N₅O₄SCuCl (unit formula wt. 412.35, chitosan unit 160.16) C, 31.89 ; H, 4.14; N, 16.90; S, 7.74, Cl 8.56%; found (for 87% DDA of chitosan) C, 30.80; H, 4.22; N, 15.48; S, 2.41%; estimated Cl, 14.20%.

Copper(II) imidazole-2-carboxaldehyde crab chitosan thiosemicarbazone (Cu-CCSIMTSC): Yield: 72%; colour: greenish yellow; m.p. > 300 °C, decomposed prior to melting; calcd. for C₁₁H₁₅N₅O₄SCuCl (unit formula wt. 412.35, chitosan unit 160.16) C, 31.89 ; H, 4.14; N, 16.90; S, 7.74, Cl 8.56%; found (for 67% DDA of chitosan) C, 31.32; H, 5.34; N, 14.35; S, 2.01%; estimated Cl, 12.78%.

Cells culturing and colorimetric MTT assays: The MDCK cell line was cultured in the complete RPMI media (mixture of 10% fetal bovine serum (FBS), 1.2% solution of antibiotics (penicillin and streptomycin), 25 mM 4-(2-hydroxyethyl)-1-piperazineethanesulfonic acid (HEPES) and an incomplete media of RPMI with glutamine) and 5% carbon dioxide for 24 h. The cells were scraped, washed well with phosphate buffer solution (PBS) to remove cellular debris, the culture medium was replaced with a fresh medium, the cells were counted and distributed with ~10⁵ cells in each well of the 96 well plate. Test solutions in dimethyl sulfoxide (DMSO) were prepared by extensive stirring and filtration of the suspension and the concentration was calculated from the weight dissolved obtainable by subtracting the weight of undissolved residue from the weight added in 10 mL of DMSO. After the incubation of 50-400 μmol L⁻¹ test solutions for 48 h with the cultured cells, the 3-(4,5-dimethylthiazol-2-yl)-2,5-diphenyltetrazolium

bromide (MTT) solution in a concentration of 5 mg/mL in PBS were added in wells. The resulting solutions were further incubated in CO₂ at 37 °C for 4 h until intracellular purple crystals of formazan were visible under microscope. The MTT was removed, formazan crystals were dissolved in DMSO, triturated and incubated in CO₂ at 37 °C for 30 min until the cells were lysed and purple crystals were dissolved. Then the intensity of the dissolved formazan crystals (purple color) was quantified using the ELISA plate reader at 551 nm. The untreated cells were taken as positive control and media only was taken as blank for the study. Cell viability percentage was obtained by the relation:

$$\text{Viable cells (\%)} = \frac{A_{\text{sample}} - A_{\text{blank}}}{A_{\text{control}} - A_{\text{blank}}}$$

Half inhibitory concentration (IC₅₀) was the concentration corresponding to the absorbance that is half of the maximum absorbance [30]. Inhibition ratio (IR) was quantified as [31]:

$$\text{IR (\%)} = \frac{A_{\text{control}} - A_{\text{sample}}}{A_{\text{control}}} \times 100$$

RESULTS AND DISCUSSION

FT-IR studies: The key FT-IR data are presented in Table-1. The broad band translocations in the spectra of both the ligands and complexes at 3500-3200 cm⁻¹ were attributed to merging of intramolecular hydrogen bonded ν(O-H) and secondary amide ν(N-H) stretches [32,33]. In addition, the ν(N-H) stretches appeared at 3200-3100 cm⁻¹ [32]. The characteristic ν(C-H) stretches were in the range of 2886-2865 cm⁻¹ [27]. The ν(NH-CS-NH) of thiosemicarbazide reported at 1550 cm⁻¹ in literature [32] was absent in the spectra of ligands. It showed the combination of NH-CS-NH group in thiosemicarbazide with C=O group of carboxaldehyde to give chitosan thiosemicarbazones. The absence of stretching vibration ν(C=O, amide I) of chitosan at about 1666 cm⁻¹ [5,6] and the appearance of ν(C=N-) bands at 1627-1619 cm⁻¹ in the ligands was the plausible indicative of the formation of imine linkage owing to condensation of amino group of chitosan with C=O group of carboxaldehyde [5,6,27,32,34,35]. The presence of medium to strong ν(C=S) bands at 1160-1072 cm⁻¹ viz. as reported literatures, ν(C=S) at 1082-1028 cm⁻¹ [36], 1112-1098 cm⁻¹ [37], 1165 cm⁻¹ [38] and the absence of ν(C-SH) band at 2600-2500 cm⁻¹ showed the existence of thiosemicarbazones in thione form [36]. Additionally, the absorption peaks in the range of 1116-1109 cm⁻¹ were attributed to the skeletal vibration of C-O-C asymmetric stretching [27]. The presence of primary ν(NH) bends in the range of 1555-1540 cm⁻¹ [32] was indicative of only partial involvement of amino group of chitosan in functionalization as chitosan thiosemicarbazone.

TABLE-1
FT-IR SPECTROSCOPIC DATA (cm⁻¹)

Compounds	ν(N-H) stretch	ν(N-H) bend	ν(C=N)	ν(C=S)	ν(C-O-C)	ν(C-H)	ν(C=N) ring
CSIMTSC	3200s	1540s	1619s	1072s	1116m	2875w	1446s
Cu-CSIMTSC	3117s	1547s	1605s	1058s	1109w	2886w	1418m
CCSIMTSC	3160s	1547s	1627s	1160m	1111s	2878w	1438s
Cu-CCSIMTSC	3103s	1555s	1602s	1150s	1111s	2865w	1417s

The negative shifts ($17\text{--}22\text{ cm}^{-1}$) of $\nu(\text{C}=\text{N})$ at $1627\text{--}1619\text{ cm}^{-1}$ in free ligands to $1605\text{--}1602\text{ cm}^{-1}$ in the corresponding complexes showed the coordination of azomethine nitrogen [39]. The negative shifts ($10\text{--}14\text{ cm}^{-1}$) of $\nu(\text{C}=\text{S})$ bands from $1160\text{--}1072\text{ cm}^{-1}$ in ligands to $1150\text{--}1058\text{ cm}^{-1}$ in complexes showed the coordination of sulphur with metal ion [36]. The imidazole ring $\nu(\text{C}-\text{N})$ stretches at $1438\text{--}1446\text{ cm}^{-1}$ in ligands [40], that also correspond to $\nu(\text{C}=\text{N})$ and $\nu(\text{C}=\text{C})$ stretches [40] were lowered to $1417\text{--}1418\text{ cm}^{-1}$ in the corresponding complexes. The lowering of these stretches by $21\text{--}28\text{ cm}^{-1}$, instead of their upward shift, was indicative of the increase in double bond character in the ring ($\text{C}=\text{N}$) bond due to resonance in the imidazole ring of ligand molecule and complex formation with lowering of these predominantly $\nu(\text{C}=\text{N})$ stretches [41]. The appearance of strong intensity peak due to imidazole ring vibration meant its presence as an active moiety [40]. The terdentate behaviour of CSIMTSC and CCSIMTSC indicated that metal-ligand charge in Cu-CSIMTSC and Cu-CCSIMTSC was balanced as a result of sulphur coordination *via* the thiolate form [42] produced due to deprotonation of $\text{H}-\text{N}-\text{C}=\text{S}$ group.

^{13}C NMR studies: The solid-state ^{13}C NMR technique has been useful to elucidate the structure of chitosan and its derivatives [43]. Polymeric structure with non-deacetylated chitin unit and chitosan thiosemicarbazone (chitosan TSC) unit with numbering of carbon atoms in the pyranose ring is shown in Fig. 2. The ^{13}C NMR spectral data are summarized in Table-2. The spectra of thiosemicarbazone ligands retained the characteristic signals due to carbon atoms in the pyranose ring of chitosan *viz.* $-\text{CH}_3$ at $\delta = 23.94\text{--}24.03$ ppm, C6 at $\delta = 62.05\text{--}62.57$ ppm, C3, C5 at $\delta = 74.53\text{--}75.83$ ppm, C4 at $\delta = 84.10\text{--}84.36$ ppm, C1 at $\delta = 104.35\text{--}105.12$ ppm [27]. The ^{13}C NMR signals at $\delta = 165$ ppm and 170 ppm have been reported to be attributed to carbon atom of $-\text{N}=\text{CH}$ group of chitosan thiosemicarbazone [27]. The literatures explain that thiosemicarbazone would be characterized by the ^{13}C NMR signal due to carbon atom of $\text{C}=\text{S}$ at $\delta = 170\text{--}180$ ppm and azomethine carbon at $\delta = 140$ ppm [44]. The signal at $\delta = 178$ ppm has been attributed to carbonyl carbon atom [27] and the superimposition of $\text{C}=\text{S}$

and $\text{C}=\text{O}$ signals has been reported to cause peak broadening [27]. In agreement to these, the azomethine carbon signal at $157.51\text{--}174.34$ ppm, $\text{C}=\text{O}$ and $\text{C}=\text{S}$ superimposition peak at $174.18\text{--}178.36$ ppm were ascertained. Additionally, the signals at $\delta = 119\text{--}162$ ppm were attributed to carbon atoms of imidazole ring [45]. Involvement of C2 towards the formation of thiosemicarbazone moiety was shown by the disappearance of C2 signal in CSIMTSC and the appearance of substituted C2 signals of the pyranose ring at 56.24 ppm in CCSIMTSC [27].

PXRD studies: The powder X-ray diffractograms of the ligands showed higher crystallinity and a shifting of standard peaks of chitosan (Joint Committee on Powder Diffraction Standards (JCPDS) # 039-1894) from 2θ at 10° and 20° to 10.69° and 18.64° in CSIMTSC and 11.66° and 19.24° in CCSIMTSC [46]. This was indicative of chemical modification of chitosan to give more ordered long-range crystallites without the complete destruction of chitosan crystallinity and the incorporation of new crystallinity in chitosan [27]. New crystallinity peaks *viz.* at $2\theta = 7.77^\circ$, 11.84° , 15.70° and 23.70° in CSIMTSC and $2\theta = 9.22^\circ$, 15.32° , 23.18° and 27.70° in CCSIMTSC were attributed to the formation of imine group and cleavage of intra-molecular hydrogen bond of chitosan [47].

Appearance of new crystalline peaks in X-ray diffractograms of the complexes showed the shifting of crystallinity pattern from chitosan thiosemicarbazone. Chelation of metal ions with different groups of thiosemicarbazone and the modification in existing crystallinity was shown by overall differences in crystallinity [47]. Further shifting of characteristic peaks derived from chitosan showed the new molecular arrangement in crystalline complexes.

Elemental microanalysis: Elemental microanalysis results and degree of substitution (DS) of chitosan thiosemicarbazones indicated the substantial extent of functionalization of chitosan as chitosan thiosemicarbazone. The values of DS [27] *viz.* 22.63% in CSIMTSC and 20.18% in CCSIMTSC showed partial introduction of Schiff base group into chitosan and more functionalization as commercial oligo chitosan thiosemicarbazones than as crab chitosan analogue. The theoretically calculated percentages of elements were based on the corresponding structures with completely deacetylated ring of chitosan, as the quantitative estimation of contributing factors to the actual structure was not possible.

Chitosan itself has been reported as a versatile ligand to coordinate through hydroxy and amino groups to copper(II) ions [29,31] in the given reaction conditions. The presence of some non-functionalized chitosan owing to partial grafting of Schiff base group into chitosan (DS $20.18\text{--}22.63\%$ with lowering of S%) has been the underlying reason to justify the formation of copper(II) chitosan complex owing to a parallel reaction of chitosan with copper(II) chloride. Moreover, this phenomenon

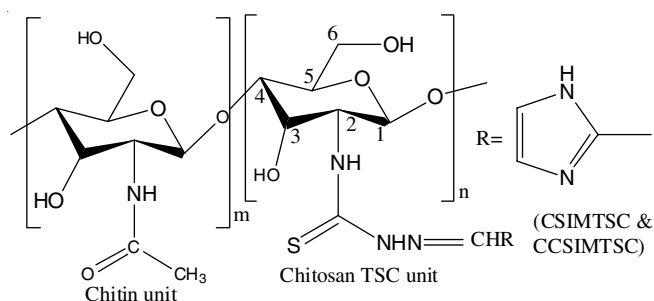


Fig. 2. Polymeric structure with non-deacetylated chitin and chitosan TSC units with numbering of carbon atoms in pyranose ring of chitosan

TABLE-2
 ^{13}C NMR SPECTRAL DATA (δ , ppm)

Compounds	CH_3	C6	C3, C5	C4	C1	Imidazole ring C	C=N	C=S, C=O superimposition
CSIMTSC	24.03	62.57	75.81	84.36	104.35	119-162	171.18	178.36
CCSIMTSC	23.91	62.05	74.53-76.84	84.10	105.12	129-157	174.34	207.58

of additional complex formation is justifiable by higher percentages of estimated chlorine than theoretically calculated chlorine percentage in copper(II) chitosan thiosemicarbazone.

The partial introduction of thiosemicarbazone was also shown by the corresponding DS values. The DS values were obviously affected by M_w of carboxaldehyde moiety in thiosemicarbazone and DDA of ring chitosan. The estimated chlorine percentages showed the coordination behaviour of chitosan thiosemicarbazone to give the complexes of proposed geometry.

Thermal studies: Thermograms (TG/DTA) of CSIMTSC and CCSIMTSC showed the thermal decomposition in three stages. The first stage was corresponding to weight loss due to loss of water viz. 7.14% weight loss at 148 °C in CSIMTSC and 7.58% weight loss at 144 °C in CCSIMTSC and this behaviour was in close agreement with 9% weight loss of chitosan at 25-150 °C due to the loss of hydrogen bonded water [47,48]. The second stage involved the abrupt increase in rate of decomposition in both (with about 44 % weight loss) from 150 °C to 350 °C indicating the onset of disruption of chitosan backbone chain. This behaviour showed an agreement with the reported degradation by 43% of chitosan backbone chain at a temperature range of 220-420 °C [47]. The third stage showed a steady increase in the rate of decomposition with more than 45% weight loss due to the disruption of backbone linkage and thermal degradation of glucosamine residue at a temperature above 400 °C [47,49].

The percentage decomposition of ligands at different temperatures (Table-3) showed a rapid rate of decomposition from 100 to 400 °C and then a steady rate of decomposition, leaving about 4% of the CSIMTSC and 6% of CCSIMTSC sample as residue of the unsaturated structure at 1000 °C. The DTA curves of both the ligands showed a steady rise up to 500 °C and a broad peak at 500-900 °C corresponding to TG weight loss in different stages.

Thermal properties of copper(II) complexes were studied by thermogravimetric analysis/differential thermal analysis/differential thermal gravimetry (TGA/DTA/DTG). The thermo-

grams of Cu-CSIMTSC and Cu-CCSIMTSC showed the thermal events at a temperature range of 25-730 °C. In comparison to ligands, TG curves of complexes showed a change in decomposition pattern with multiple stages of weight loss. There was an increase in the rate of decomposition corresponding to disruption of chitosan backbone chain observed at a temperature range of 100-300 °C with a weight loss of 23% in Cu-CSIMTSC and 19% in Cu-CCSIMTSC. Thermal degradation of glucosamine residue was observed at 500-600 °C with a weight loss of 21% in Cu-CSIMTSC and at a temperature range of 300-400 °C with an abrupt weight loss of 54% in Cu-CCSIMTSC [47,49]. In Cu-CSIMTSC, the DTA curve showed a steady rise up to 450 °C and broad exothermic peak in the temperature range of 450-560 °C, while in Cu-CCSIMTSC, the DTA curve showed a steady rise up to 300 °C and an exothermic peak in the temperature range of 300-400 °C. The percentage decomposition of complexes at different temperatures (Table-4) showed a steady rate of decomposition after 600 °C leaving about 22% of the sample as residue of the unsaturated structure at 700 °C in Cu-CSIMTSC, while there was a steady rate of decomposition after 500 °C leaving about 15% of sample as residue at 700 °C in Cu-CCSIMTSC.

The DTG curves further supported the above-mentioned stages of thermal decomposition with a weight loss of 0.27 mg/min at 257 °C, 0.50 mg/min at 546 °C in Cu-CSIMTSC and 1.26 mg/min at 106 °C in Cu-CCSIMTSC. Overall, the thermal data showed substantial stability of copper(II) complexes.

Magnetic susceptibility measurement and electron paramagnetic resonance (EPR) studies: Magnetic susceptibility measurement and g values in EPR spectra of the complexes are summarized in Table-5. Magnetic susceptibility measurement ($T = 298$ K, $R_0 = -34$, $L = 1.5$ cm) showed the effective magnetic moment (μ_{eff}) values in the range of 1.87-1.89 B.M. which are close to spin-only moment of 1.73 B.M. due to an unpaired electron. This indicated a low spin-spin coupling between unpaired electrons of different copper atoms [50] and some increase in the moment was attributed to large spin orbit coupling constant

TABLE-3
THERMAL STUDIES OF LIGANDS: PERCENTAGE DECOMPOSITION AT DIFFERENT TEMPERATURES

Temperature (°C)	100	200	300	400	500	600	700	800	900	1000
CSIMTSC: % decomposition	5	12	44	52	60	68	76	83	88	96
CCSIMTSC: % decomposition	6	18	45	51	60	69	72	81	90	94

TABLE-4
THERMAL STUDIES OF COMPLEXES: PERCENTAGE DECOMPOSITION AT DIFFERENT TEMPERATURES

Temperature (°C)	100	200	300	400	500	600	700
Cu-CSIMTSC: % decomposition	8	13	31	37	46	67	78
Cu-CCSIMTSC: % decomposition	4	8	24	78	83	84	85

TABLE-5
MAGNETIC SUSCEPTIBILITY MEASUREMENT AND g VALUE IN EPR SPECTRA OF COMPLEXES

Complexes	Magnetic susceptibility measurement				g value in EPR spectra
	χ_g	M_w	χ_m	μ_{eff} (BM)	
Cu-CSIMTSC	3.55×10^{-6}	412.35	0.0015	1.89	2.100
Cu-CCSIMTSC	3.40×10^{-6}	412.35	0.0014	1.87	2.096

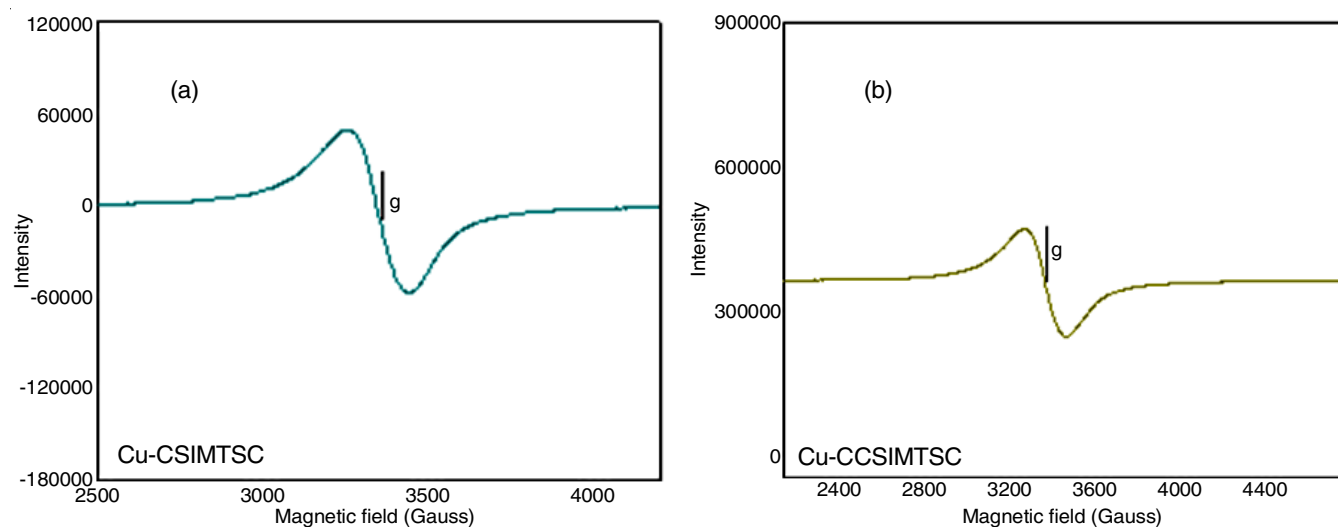


Fig. 3. EPR spectra of complexes (a) Cu-CSIMTSC, (b) Cu-CCSIMTSC

of cupric ion [51]. Magnetic moment of < 1.90 B.M. indicated the square planar or octahedral stereochemistry of the complexes [52].

The EPR spectra of complexes (Fig. 3) were characterizable by axial g tensors [53] and the non-resolution of hyperfine features due to copper ($S = 1/2$ and $I = 3/2$) was owing to intermolecular spin-spin interactions and dimeric association of molecules [54,55]. It meant that the absence of hyperfine splitting was attributed to exchange broadening due to still incomplete separation of paramagnetic centres [56] at a low X-band frequency of 9.8 GHz [56]. The spectra corresponding to an unpaired electron in $d_{x^2-y^2}$ orbital of Cu(II) centres were in agreement with a square planar geometry [57], but the g parallel tensors were undetectable due to absence of hyperfine splitting. The shifting of g value from g_e (2.0023) that is due to spin orbital coupling of metal orbitals with unpaired electrons has been reported to depend upon the degree of covalency of the complex that is determined by the unpaired electron density at the donor atoms of ligand molecule [50]. The absence of half field peak at 1500 Gauss suggesting the absence of two copper centres in the same lacuna indicated the mononuclear structure of the complexes [58].

On the basis of the aforementioned results, the copper(II) complexes were proposed to assume the mononuclear distorted square planar geometry (Fig. 4). The thione sulphur, azomethine nitrogen and heterocyclic nitrogen atom of imidazole-2-carboxaldehyde based chitosan thiosemicarbazone and one chlorine atom were used as the donor sites in coordination with copper(II) ion in the complexes.

Antitumorigenic activity: The MDCK cell line, unlike the early non-tumorigenic cell populations [58], was propagated with the expression of immortalization and tumorigenic phenotype upon the culture in complete media. The literature has shown the development of tumorigenicity and the use of tumorigenic canine cell lines, but the mechanism of neoplastic transformation in mammalian cells is yet unclear [59]. The antitumorigenic profile against MDCK cell line by chitosan thiosemicarbazones and their copper(II) complexes is presented

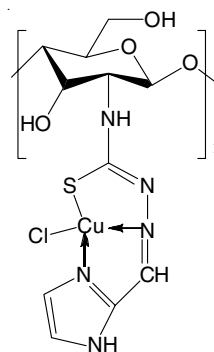


Fig. 4. Proposed structure of complexes: Cu-CSIMTSC and Cu-CCSIMTSC

in Table-6. Oligo chitosan thiosemicarbazone showed higher antiproliferative activity with IC_{50} value of $170.46 \mu\text{mol L}^{-1}$ in CSIMTSC, but its crab shell chitosan analogue CCSIMTSC showed low antitumorigenic activity with 52-70% cell viability on raising the concentration to $400 \mu\text{mol L}^{-1}$. There was concentration dependent rise in IR% and at a given concentration, oligo chitosan thiosemicarbazone showed more inhibition of cell growth. The data showed cytotoxicity enhancement upon the complex formation of chitosan thiosemicarbazones.

TABLE-6
ANTITUMORIGENIC PROFILE AGAINST MDCK
CELL LINE BY CHITOSAN THIOSEMICARBAZONES
AND THEIR COPPER(II) COMPLEXES

Compounds	Cell viability % (at 50-400 $\mu\text{mol L}^{-1}$)	IR % (at 50-400 $\mu\text{mol L}^{-1}$)
CSIMTSC	78-24 ($IC_{50} = 170.46$)	22-76
CCSIMTSC	72-70	28-30
Cu-CSIMTSC	59-43 ($IC_{50} = 117.86$)	41-57
Cu-CCSIMTSC	81-49 ($IC_{50} = 387.20$)	19-51

Conclusion

The semi synthetic tailoring of imidazole-2-carboxaldehyde chitosan thiosemicarbazones and their copper(II) complexes was critical towards the chemical modification of chitosan to get its antitumorigenic derivatives. All the derivatives showed

inhibitory effect on tumorigenic MDCK cell line proliferation and the oligo chitosan derivatives were more remarkable. Complex formation caused the increase in antitumorigenic activity of chitosan thiosemicarbazones. The factors such as degree of deacetylation (DDA) and molecular weight (M_w) of chitosan, degree of grafting of thiosemicarbazone group in chitosan, mode of coordination to copper(II) ion and low solubility in the selected solvent could have severe effect on anticancer activity of these chitosan derivatives. Overall, the moderate anti-proliferative activity of these newly synthesized biomaterials against the tumorigenic cell line presents the area of further investigation towards the safety profiles in normal cells and higher activity against the cancer cell lines.

ACKNOWLEDGEMENTS

Nepal Academy of Science and Technology (NAST) and Indian National Science Academy (INSA) are duly acknowledged for a Ph.D. fellowship and research exchange fellowship to Hari Sharan Adhikari. The authors are thankful to Prof. A.R. Chakravarty, Indian Institute of Science, Bangalore, India for recommendation in INSA, Dr. Agni Koirala, Sogang University, Department of Chemistry, Korea Center for Artificial Photosynthesis, Centre for Nanomaterial, Shinsudong, South Korea for EPR data and Dr. Ravinder Kumar Choudhary, Department of Chemistry, Gurukula Kangri Vishwavidyalaya, Haridwar, India for thermal analysis. The authors also acknowledge Central Department of Biotechnology, Tribhuvan University, Kathmandu, Nepal and the Head of the Department, Prof. Dr. Krishna Das Manandhar for arrangement of biological screening against the MDCK cell line.

CONFLICT OF INTEREST

The authors declare that there is no conflict of interests regarding the publication of this article.

REFERENCES

- I. Aranaz, M. Mengibar, R. Harris, I. Paños, B. Miralles, N. Acosta, G. Galed and Á. Heras, *Curr. Chem. Biol.*, **3**, 203 (2009); <https://doi.org/10.2174/2212796810903020203>
- R.C.F. Cheung, T.B. Ng, J.H. Wong and W.Y. Chan, *Mar. Drugs*, **13**, 5156 (2015); <https://doi.org/10.3390/md13085156>
- S. Pokhrel and P.N. Yadav, *J. Macromol. Sci. A*, **56**, 450 (2019); <https://doi.org/10.1080/10601325.2019.1581576>
- H.S. Adhikari and P.N. Yadav, *Int. J. Biomater.*, **2018**, 1 (2018); <https://doi.org/10.1155/2018/2952085>
- R. Saud, S. Pokhrel and P.N. Yadav, *J. Macromol. Sci. A*, **56**, 375 (2019); <https://doi.org/10.1080/10601325.2019.1578616>
- M.K. Yadav, S. Pokhrel and P.N. Yadav, *J. Macromol. Sci. A*, **57**, 703 (2020); <https://doi.org/10.1080/10601325.2020.1763809>
- A.S. Montaser, A.R. Wassel and O.N. Al-Shaye'a, *Int. J. Biol. Macromol.*, **124**, 802 (2019); <https://doi.org/10.1016/j.ijbiomac.2018.11.229>
- Y. S. Wimaradhani, D. F. Suniarti, H. J. Freisleben, S.I. Wanandi, N. C. Siregar and M.-A. Ikeda, *J. Oral Sci.*, **56**, 119 (2014); <https://doi.org/10.2334/josnusd.56.119>
- J.K. Park, M.J. Chung, H.N. Choi and Y.I. Park, *Int. J. Mol. Sci.*, **12**, 266 (2011); <https://doi.org/10.3390/ijms12010266>
- L. Qi, Z. Xu, X. Jiang, C. Hu and X. Zou, *Carbohydr. Res.*, **339**, 2693 (2004); <https://doi.org/10.1016/j.carres.2004.09.007>
- Z. Zhong, Z. Zhong, R. Xing, P. Li and G. Mo, *Int. J. Biol. Macromol.*, **47**, 93 (2010); <https://doi.org/10.1016/j.ijbiomac.2010.05.016>
- J.M. McCord, *Am. J. Med.*, **108**, 652 (2000); [https://doi.org/10.1016/S0002-9343\(00\)00412-5](https://doi.org/10.1016/S0002-9343(00)00412-5)
- A.L. Rao, M. Bharani and V. Pallavi, *Adv. Pharmacol. Toxicol.*, **7**, 29 (2006).
- W. Xie, P. Xu and Q. Liu, *Bioorg. Med. Chem. Lett.*, **11**, 1699 (2001); [https://doi.org/10.1016/S0960-894X\(01\)00285-2](https://doi.org/10.1016/S0960-894X(01)00285-2)
- I. Ali, M.N. Lone and H.Y. Aboul-Enein, *MedChemComm*, **8**, 1742 (2017); <https://doi.org/10.1039/C7MD00067G>
- B. Shakya and P.N. Yadav, *Mini Rev. Med. Chem.*, **20**, 638 (2020); <https://doi.org/10.2174/1389557519666191029130310>
- B. Shakya, P.N. Yadav, J.-Y. Ueda and S. Awale, *Bioorg. Med. Chem. Lett.*, **24**, 458 (2014); <https://doi.org/10.1016/j.bmcl.2013.12.044>
- J. Easmon, G. Pürstinger, G. Heinisch, T. Roth, H.H. Fiebig, W. Holzer, W. Jäger, M. Jenny and J. Hofmann, *J. Med. Chem.*, **44**, 2164 (2001); <https://doi.org/10.1021/jm000979z>
- M.N.M. Milunovic, E.A. Enyedy, N.V. Nagy, T. Kiss, R. Trondl, M.A. Jakupc, B.K. Keppler, R. Krachler, G. Novitchi and V.B. Arion, *Inorg. Chem.*, **51**, 9309 (2012); <https://doi.org/10.1021/ic300967j>
- B.M. Zeglis, V. Divilov and J.S. Lewis, *J. Med. Chem.*, **54**, 2391 (2011); <https://doi.org/10.1021/jm101532u>
- S. Adsule, V. Barve, D. Chen, F. Ahmed, Q.P. Dou, S. Padhye and F.H. Sarkar, *J. Med. Chem.*, **49**, 7242 (2006); <https://doi.org/10.1021/jm060712l>
- O. Palamarcu, M.N.M. Milunovic, A. Sirbu, E. Stratulat, A. Pui, N. Gligorijevic, S. Radulovic, J. Kozisek, D. Darvasiova, P. Rapta, E.A. Enyedy, G. Novitchi, S. Shova and V.B. Arion, *New J. Chem.*, **43**, 1340 (2019); <https://doi.org/10.1039/C8NJ04041A>
- R.L. Omeir, B. Teferedegne, G.S. Foseh, J.J. Beren, P.J. Snoy, L.R. Brinster, J.L. Cook, K. Peden and A.M. Lewis Jr., *Comp. Med.*, **61**, 243 (2011).
- P. Tuangpholkrung, C. Muanprasat and V. Chatsudthipong, *The FASEB J.*, **31**, 1032.6 (2018); https://doi.org/10.1096/fasebj.31.1_supplement.1032.6
- S. Moradi Dehaghi, B. Rahmanifar, A.M. Moradi and P.A. Azar, *J. Saudi Chem. Soc.*, **18**, 348 (2014); <https://doi.org/10.1016/j.jscs.2014.01.004>
- Y.Q. Zhang, C.H. Xue, Y. Xue, R.C. Gao and X.L. Zhang, *Carbohydr. Res.*, **340**, 1914 (2005); <https://doi.org/10.1016/j.carres.2005.05.005>
- Y. Qin, R. Xing, S. Liu, K. Li, X. Meng, R. Li, J. Cui, B. Li and P. Li, *Carbohydr. Polym.*, **87**, 2664 (2012); <https://doi.org/10.1016/j.carbpol.2011.11.048>
- M.A. Demertzis, P.N. Yadav and D. Kovala-Demertzi, *Helv. Chim. Acta*, **89**, 1959 (2006); <https://doi.org/10.1002/hlca.200690187>
- X. Wang, Y. Du, L. Fan, H. Liu and Y. Hu, *Polym. Bull.*, **55**, 105 (2005); <https://doi.org/10.1007/s00289-005-0414-1>
- P. Kumar, A. Nagarajan and P.D. Uchil, *Cold Spring Harb. Protoc.*, **2018**, 469 (2018); <https://doi.org/10.1101/pdb.prot095505>
- Y. Zheng, Y. Yi, Y. Qi, Y. Wang, W. Zhang and M. Du, *Bioorg. Med. Chem. Lett.*, **16**, 4127 (2006); <https://doi.org/10.1016/j.bmcl.2006.04.077>
- Z. Zhong, B. Aotegen and H. Xu, *Int. J. Biol. Macromol.*, **48**, 713 (2011); <https://doi.org/10.1016/j.ijbiomac.2011.01.029>
- S. Sashikala and S.S. Shafi, *Der Pharm. Lett.*, **6**, 90 (2014).
- H. Abdelwahab, S. Hassan, G. Yacout, M. Mostafa and M. El Sadek, *Polymer*, **7**, 2690 (2015); <https://doi.org/10.3390/polym7121532>
- V.L. Triana-Guzmán, Y. Ruiz-Cruz, E.L. Romero-Peñaloza, H.F. Zuluaga-Corralles and M.N. Chaur-Valencia, *Rev. Fac. Ing. Univ. Antioquia*, **89**, 34 (2018); <https://doi.org/10.17533/udea.redin.n89a05>

36. N. Bharti, Shailendra, S. Sharma, F. Naqvi and A. Azam, *Bioorg. Med. Chem.*, **11**, 2923 (2003); [https://doi.org/10.1016/S0968-0896\(03\)00213-X](https://doi.org/10.1016/S0968-0896(03)00213-X)
37. S. Sharma, F. Athar, M.R. Maurya and A. Azam, *Eur. J. Med. Chem.*, **40**, 1414 (2005); <https://doi.org/10.1016/j.ejmech.2005.05.013>
38. K. Alomar, M.A. Khan, M. Allain and G. Bouet, *Polyhedron*, **28**, 1273 (2009); <https://doi.org/10.1016/j.poly.2009.02.042>
39. B. Singh and H. Mishra, *J. Indian Chem. Soc.*, **63**, 692 (1986).
40. A. Madanagopal, S. Periandy, P. Gayathri, S. Ramalingam, S. Xavier and V. K. Ivanov, *J. Taibah Univ. Sci.*, **11**, 975 (2017); <https://doi.org/10.1016/j.jtusc.2017.02.006>
41. A.S. Munde, A.N. Jagdale, S.M. Jadhav and T.K. Chondhekar, *J. Korean Chem. Soc.*, **53**, 407 (2009); <https://doi.org/10.5012/jkcs.2009.53.4.407>
42. M. Joseph, V. Suni, M.R. Prathapachandra Kurup, M. Nethaji, A. Kishore and S.G. Bhat, *Polyhedron*, **23**, 3069 (2004); <https://doi.org/10.1016/j.poly.2004.09.026>
43. A.A. De Angelis, D. Capitani and V. Crescenzi, *Macromolecules*, **31**, 1595 (1998); <https://doi.org/10.1021/ma971619x>
44. M.A. El-Atawy, A.Z. Omar, M. Hagar and E.M. Shashira, *Green Chem. Lett. Rev.*, **12**, 364 (2019); <https://doi.org/10.1080/17518253.2019.1646813>
45. K. Bouchmella, S.G. Dutremez, B. Alonso, F. Mauri and C. Gervais, *Cryst. Growth Des.*, **8**, 3941 (2008); <https://doi.org/10.1021/cg700975v>
46. R. Ramya, P.N. Sudha and J. Mahalakshmi, *Int. J. Scient. Res. Publ.*, **2(10)**, 1 (2012).
47. T.F. Jiao, J. Zhou, J.-X. Zhou, L.-H. Gao, Y.Y. Xing and X.-H. Li, *Iran. Polym. J.*, **20**, 123 (2011).
48. X.X. Jin, J.T. Wang and J. Bai, *Carbohydr. Res.*, **344**, 825 (2009); <https://doi.org/10.1016/j.carres.2009.01.022>
49. M.N. Khalid, F. Agnely, N. Yagoubi, J.L. Grossiord and G. Couarraze, *Eur. J. Pharm. Sci.*, **15**, 425 (2002); [https://doi.org/10.1016/S0928-0987\(02\)00029-5](https://doi.org/10.1016/S0928-0987(02)00029-5)
50. A. Ahmed and R.A. Lal, *Arab. J. Chem.*, **10**, S901 (2017); <https://doi.org/10.1016/j.arabjc.2012.12.026>
51. C. Djordjevic, *Croat. Chem. Acta*, **32**, 183 (1960).
52. B.N. Figgis, *Nature*, **182**, 1568 (1958); <https://doi.org/10.1038/1821568a0>
53. T.H. Bennur, D. Srinivas and P. Ratnasamy, *Micropor. Mesopor. Mater.*, **48**, 111 (2001); [https://doi.org/10.1016/S1387-1811\(01\)00345-6](https://doi.org/10.1016/S1387-1811(01)00345-6)
54. M.M. Bhadbhade and D. Srinivas, *Inorg. Chem.*, **32**, 5458 (1993); <https://doi.org/10.1021/ic00076a010>
55. E. Suresh, M.M. Bhadbhade and D. Srinivas, *Polyhedron*, **15**, 4133 (1996); [https://doi.org/10.1016/0277-5387\(96\)00178-7](https://doi.org/10.1016/0277-5387(96)00178-7)
56. R. Farra, K. Thiel, A. Winter, T. Klamroth, A. Poppl, A. Kelling, U. Schilde, A. Taubert and P. Strauch, *New J. Chem.*, **35**, 2793 (2011); <https://doi.org/10.1039/c1nj20271e>
57. E. Garribba and G. Micera, *J. Chem. Educ.*, **83**, 1229 (2006); <https://doi.org/10.1021/ed083p1229>
58. A. Patel and R. Sadasivan, *Inorg. Chim. Acta*, **458**, 101 (2017); <https://doi.org/10.1016/j.ica.2016.12.031>
59. R. Omeir, R. Thomas, B. Teferedegne, C. Williams, G. Foseh, J. Macauley, L. Brinster, J. Beren, K. Peden, M. Breen and A.M. Lewis Jr., *Chromosome Res.*, **23**, 663 (2015); <https://doi.org/10.1007/s10577-015-9474-8>